

## RalBP1 Is Necessary for Metastasis of Human Cancer Cell Lines<sup>1</sup>

Zhong Wu\*, Charles Owens\*, Nidhi Chandra\*, Kay Popovic<sup>†</sup>, Mark Conaway<sup>‡</sup> and Dan Theodorescu<sup>\*,§</sup>

\*Department of Molecular Physiology and Biological Physics, University of Virginia, Charlottesville, VA, USA; <sup>†</sup>Department of Radiology, University of Virginia, Charlottesville, VA, USA; <sup>‡</sup>Department of Public Health Sciences (Biostatistics), University of Virginia, Charlottesville, VA, USA; <sup>§</sup>Paul Mellon Prostate Cancer Institute, University of Virginia, Charlottesville, VA, USA

### Abstract

RalA expression in human prostate cancer is associated with cell migration and is necessary for bone metastasis. However, the downstream effectors of RalA that mediate these functions remain unclear. Here we examined cell migration after small interfering RNA–mediated depletion of Ral effectors Ral binding protein 1 (RalBP1/RLIP), exocyst complex component 2 (Sec5), and phospholipase D1 (PLD1) and found that RalBP1 and RalA depletion inhibited cell migration to a similar extent. Stable lentivirus short hairpin interfering RNA–mediated depletion of RalA and RalBP1 in PC3 human prostate cancer cells inhibited bone metastasis after intracardiac inoculation. Depletion of RalBP1 diminished orthotopic tumor growth of PC3 cells and inhibited spontaneous metastasis from this site. Interestingly, the expression of wild-type or RalA mutants deficient in RalBP1 binding was effective at rescuing the reduced metastatic capacity of RalA-depleted PC3 cells, suggesting that RalA depletion does not reduce this solely by diminished interaction with RalBP1. To determine whether the role of RalBP1 in metastasis is relevant beyond prostate cancer, we studied the requirement of RalBP1 expression in an experimental metastasis model of human bladder cancer, a tumor type with high RalBP1 expression. Depletion of RalBP1 in UMUC3 cells resulted in decreased lung colonization while having a minimal effect on subcutaneous tumor growth. Our studies are the first to suggest that the expression of RalBP1 is necessary for human cancer cell metastasis. Furthermore, we show that the requirement for RalA expression for manifestation of this phenotype is not entirely dependent on a RalA-RalBP1 interaction.

*Neoplasia* (2010) 12, 1003–1012

### Introduction

RalA and RalB GTPases are monomeric G proteins of the Ras superfamily with 82% amino acid identity [1]. Ral proteins were initially implicated in Ras-mediated transformation of human cells [2] as well as in maintenance of the Ras-driven malignant phenotype [3]. Recent evidence also indicates their essential role in cancer progression and metastasis. Both RalA and RalB have been shown to be involved in pancreatic cancer cell metastasis [4]. In contrast, RalA but not RalB was necessary for prostate cancer PC3 cells to metastasize to bone after stable expression of RNA interference for Ral paralogs [5]. We recently observed that RalA expression in bladder tumors is associated with higher stage [6]. Experimentally, RalA and RalB depletion after transient small interfering RNA (siRNA)–mediated knockdown was associated with decreased cell growth and migration in both bladder and

prostate cancer cells [7]. However, the downstream signaling pathways that mediate Ral function in migration and metastasis are unclear.

On activation, Ral paralogs bind to several effectors including RalBP1 (RLIP), exocyst components (Sec5 and Exo84), filamin,

Address all correspondence to: Dan Theodorescu, MD, PhD, University of Colorado Comprehensive Cancer Center, University of Colorado, 13001 E 17th Pl MS #F-434, Aurora, CO 80045. E-mail: dan.theodorescu@ucdenver.edu

<sup>1</sup>This work was supported by a National Institutes of Health award CA104106 to D.T. The authors declare that they have no competing financial interests.

Received 31 July 2010; Revised 11 September 2010; Accepted 15 September 2010

Copyright © 2010 Neoplasia Press, Inc. All rights reserved 1522-8002/10/\$25.00  
DOI 10.1593/neo.101080

phospholipase D1 (PLD1), and ZONAB, and this results in diverse Ral-associated functions [1]. RalBP1 is the best-characterized Ral effector, and previous results suggested its association with Ral-mediated tumorigenesis [3]. Furthermore, expression of RalBP1 is increased in human bladder cancer tissues compared with normal tissues, and its level was correlated with Ral expression [6]. Depletion of RalBP1 by antisense or inhibition of its function by antibody decreased subcutaneous xenograft tumor growth in a number of cancer cell lines [8,9]. Similar to RalBP1, the exocyst complex component Sec5 has been shown to be involved in Ral-mediated transformation [3]. PLD1 was also associated with cells transformation by oncogenes including *Ras* [10,11].

Although these Ral effectors have been implicated in transformation, their functional role in Ral-mediated cancer progression has not been clearly defined. Here, we begin by examining the function of Ral effectors on cell migration and find that RalBP1 depletion inhibited cell migration to a similar extent as RalA depletion did in human prostate cancer cells. Further examination of the consequences of stable depletion of RalBP1 in prostate and bladder cancer cells points to an important role for RalBP1 in cancer metastasis.

## Materials and Methods

### Cell Culture and Counting

Human bladder cancer UMUC3 and prostate cancer PC-3 cell lines were obtained from American Type Culture Collection (Rockville, MD), and cultures were as described. For counting assays, cells were plated at a concentration of 1000 cells per well in 200  $\mu$ l in 96-well tissue culture plates (Corning Incorporated, Corning, NY). Replicate plates were plated for each indicated time point. At each time point, 10  $\mu$ l of Alamar blue was added to each well, and fluorescence was measured 4 hours later on a microplate reader (BioTek, Winooski, VT) with excitation at 520 nm and emission at 570 nm.

### Short Hairpin Interfering RNA and siRNA Reagents and Transfection

The NH<sub>2</sub>-terminally Flag-tagged RalA expression pFlag-CMV-4 vector was described previously [7]. The RalA sequence 5'-CGATGAGTTTGTGGAGGACT-3' was targeted by short hairpin interfering RNA (shRNA). Lentiviral shRNA expression vectors targeting RalA, RalB, and RalBP1 were purchased from Sigma (St Louis, MO). RalA-5 shRNA (5'-CCGGCGATGAGTTTGTGGAGGACTACTCGAGTAGTCCACAACTCATCGTTTTT-3'), RalB-4 shRNA (CCGGCCTTTACAGCAACTGCCGAATCTCGAGATTTCGGCAGTTGCTGTAAAGTTTTT), RalBP1-1 shRNA (5'-CCGGCCAGAGAATTTGCTTACCAAACTCGAGTTTGGTAAGCAAATTTCTCTGGTTTTT-3'), and RalBP1-3 shRNA (5'-CCGGGCACAAGAGATAGCCAGTCTTCTCGAGAA-GACTGGCTATCTCTGTGCTTTTTG-3') were encoded in a lentiviral expression vector, PLKO, which carries a puromycin selection marker. The same lentiviral vector containing a nontarget shRNA sequence that does not target any human gene was used as control. The SFGnesTGL vector expressing a thymidine kinase/green fluorescent protein/luciferase (TGL) fusion protein was described [12]. All plasmid DNA used for transfection was prepared by the "EndoFree Plasmid Maxi kit" from Qiagen (Valencia, CA).

siRNA duplexes were purchased from Dharmacon (Lafayette, CO). RalA targeting siRNA was described previously [7]. RalBP1-targeting siRNA duplexes were a mixture of two individual duplex with the following targeting sequence: 5'-GAACGAAGAGCUGAAUAUU-3'

and 5'-GAAGGCAUCUACAGAGUAUUU-3'. siRNA duplexes targeting Sec5 and PLD1 were smart pools, and the siRNA duplex targeting luciferase (GL2), 5'-CGTACGCGAATACTTCGA-3', was used as control siRNA. Transfection of cells with siRNA duplexes (100 nM) was done using OligofectAMINE (Invitrogen, Carlsbad, CA).

### Establishment of Luciferase-Expressing Stable Knockdown or Overexpressing Cells

Parental UMUC3 and PC3 cells were stably transfected with linearized SFGnesTGL vector, and luciferase-expressing cells were selected by fluorescence-activated cell sorting of green fluorescent protein. To generate stable RalA and RalBP1 knockdown cells, RalA and RalBP1 shRNA constructs were cotransfected with lentiviral package plasmids CMV $\Delta$ R8.2 and pMD.G into 293T cells. Viral particles harvested 48 hours after transfection were used to infect luciferase-expressing UMUC3 and PC3 cells. Positive cells were selected with 2  $\mu$ g/ml puromycin, and the knockdown of Ral and RalBP1 was confirmed by Western blots. To make stable RalA and RalBP1 expression PC3 cells, flag-tagged wild-type RalA, D49N mutant RalA, RalBP1, and flag vector control were stably transfected into luciferase-expressing PC3 cells. These constructs had silent mismatch mutations that allowed them to be expressed despite the presence of shRNA. After 1 mg/ml G418 selection, pools of positive cells were confirmed with Western blots.

### Cell Chemotaxis and Plating Efficiency Assays

PC3 cells were transfected with siRNA oligo duplexes to transiently knockdown of RalA, RalBP1, Sec5, and PLD1. Cells were harvested 72 hours after transfection and counted in a hemacytometer and were resuspended in serum-free Dulbecco modified Eagle medium (DMEM)/F12 medium. Cells (20,000) were added in triplicate to the upper chamber of transwell filters (8.0  $\mu$ m pores; Becton Dickinson, Franklin Lakes, NJ) in a 24-well tissue culture plate. The lower chambers contained 0.65 ml of DMEM/F12 with 2% FBS. For plating control, same number of cells was added in duplicate in wells of 96-well plate (roughly the same growth area compared with the upper chamber of transwell) containing 50  $\mu$ l of DMEM/F12 medium with 2% FBS. After 20 hours of plating, cells remaining on the upper surface of the filters were removed with cotton swabs, and cells on the lower surface were fixed with 100% methanol, stained with crystal violet, and counted with the aid of a grid coverslip (Bellco Biotechnology, Vineland, NJ). Cell numbers in plating control wells of 96-well plates were determined with CyQuant (Invitrogen) according to manufacturer's instructions.

### Real-time Reverse Transcription-Polymerase Chain Reaction Analysis

Real-time reverse transcription-polymerase chain reaction (RT-PCR) was carried out on iCycler Optical Module (Bio-Rad, Hercules, CA) with IQ SYBR Green (Bio-Rad) fluorescent dye included in the PCR to determine the amount of messenger RNA (mRNA) level for RalA, RalBP1, Sec5, and PLD1. Primers used for RalA were forward 5'-CAGACAGCTATCGGAAGAAG-3' and reverse 5'-AGAAAACACAGAGGAACCCC-3'. Primers for RalBP1 were forward 5'-ACGGGAGGAGTCTACAAAC-3' and reverse 5'-CCTCTTCAAATCTGGGCATA-3'. Primers for Sec5 were forward 5'-ATGTCCTC-ACTTGGGTCAT-3' and reverse 5'-GCTCGCTCACGCCATC-CAG-3'. Primers for PLD1 were forward 5'-CAGAGCTTGGTAAT-CAGTGG-3' and reverse 5'-GCGGTCATTTATGTTGGCAG-3'. Real-time RT-PCR for glucuronidase  $\beta$  (*Gusb*) was used as an internal

control, and primers were forward 5'-CCGACTTCTCTGACAACC-GACG-3' and reverse 5'-AGCCGACAAAATGCCGCAGACG-3'. Expression levels of RalA, RalBP1, Sec5, and PLD1 were normalized to the expression of glucuronidase  $\beta$  in each sample by calculating the ratio of individual gene expression to Gusb expression.

### Western Blot Analysis

Protein extracts were prepared from stable Ral- and RalBP1-depleted UMUC3 and PC3 cells. Western blots were carried out as described

[13] using commercial chemiluminescence reagents (SuperSignal West Femto; Pierce, Rockford, IL) and  $\alpha$ -imaging (Alpha Innotech, San Leandro, CA). The anti-RalA monoclonal antibody was purchased from BD Transduction Laboratory (Franklin Lakes, NJ) and used at 1:1000 dilution. The polyclonal anti-RalBP1 (Abnova, Walnut, CA) antibody was used at 1:2000 dilution. The monoclonal anti- $\alpha$ -tubulin antibody was purchased from Oncogene (San Diego, CA) and was diluted at 1:2000. The HRP-conjugated antimouse and antirabbit secondary antibodies were both from Pierce and were used at 1:2500

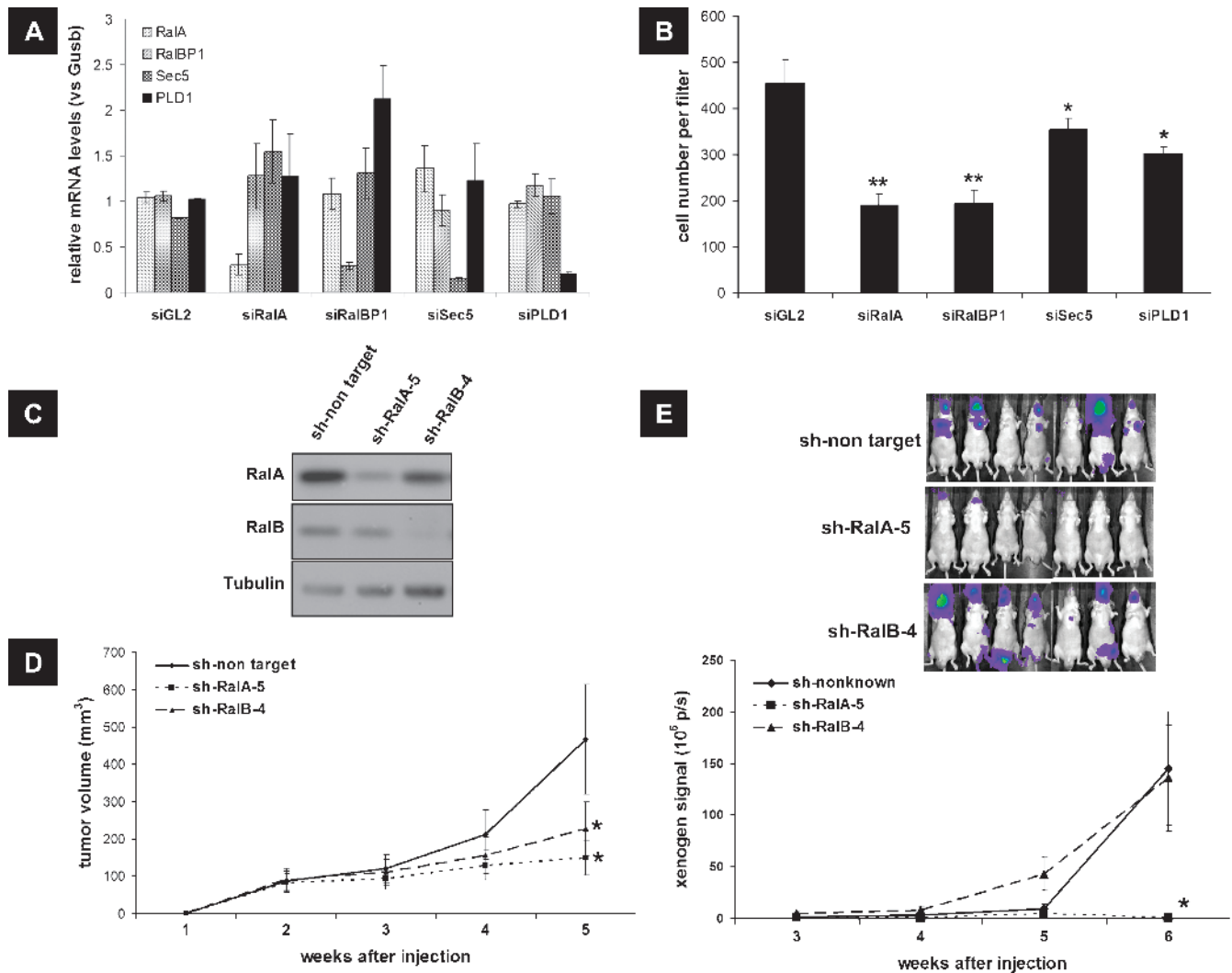


**Figure 1.** *In vitro* and *in vivo* PC3 characterization after depletion of Ral and its effectors. (A) mRNA expression levels of Ral and effectors 72 hours after transient siRNA transfection of PC3 cells with siRNA targeting RalA, RalBP1, Sec5, and PLD1. Cells were lysed for RNA extraction, and expression levels were quantitated by RT-PCR with primers specific for RalA, RalBP1, Sec5, and PLD1. Expression levels were normalized with glucuronidase- $\beta$  (Gusb) by calculating the ratio between individual gene expression and Gusb expression as described in Materials and Methods. (B) Duplicate plate transfected with siRNA was harvested at 72 hours after transfection, and  $2 \times 10^4$  cells were plated in the upper compartment of a Boyden chamber in serum-free medium, whereas 2% FBS-containing medium was added into the bottom compartment. Cells were allowed to migrate for 20 hours. Statistical significance compared with siGL2 control siRNA was indicated by \* $P < .05$  and \*\* $P < .01$ . (C) Western blots demonstrating decreased RalA and RalB protein levels in PC3 cells after infection of lentiviral-based RalA and RalB targeting shRNA constructs shRalA-5 and shRalB-4. (D) Subcutaneous tumor growth of non-target shRNA PC3 tumors and RalA as well as RalB knockdown tumors. PC3 cells in serum-free RPMI medium were mixed with Matrigel and were subcutaneously injected into the mouse flank region in 10 mice per group with two sites per mouse. Tumor volume was measured every week with calipers. \* $P < .05$  compared with sh-nontarget control at 5 weeks. (E) Xenogen evaluation of metastatic tumor growth of mice injected with either nontarget shRNA or RalA- and RalB-targeting shRNA PC3 cells. Xenogen images shown were taken at 6 weeks after injection in seven mice per group. Graphs indicate quantitation of total-body Xenogen signals at 3, 4, 5, and 6 weeks after injection. \* $P < .05$  compared with sh-nontarget control at 5 weeks.

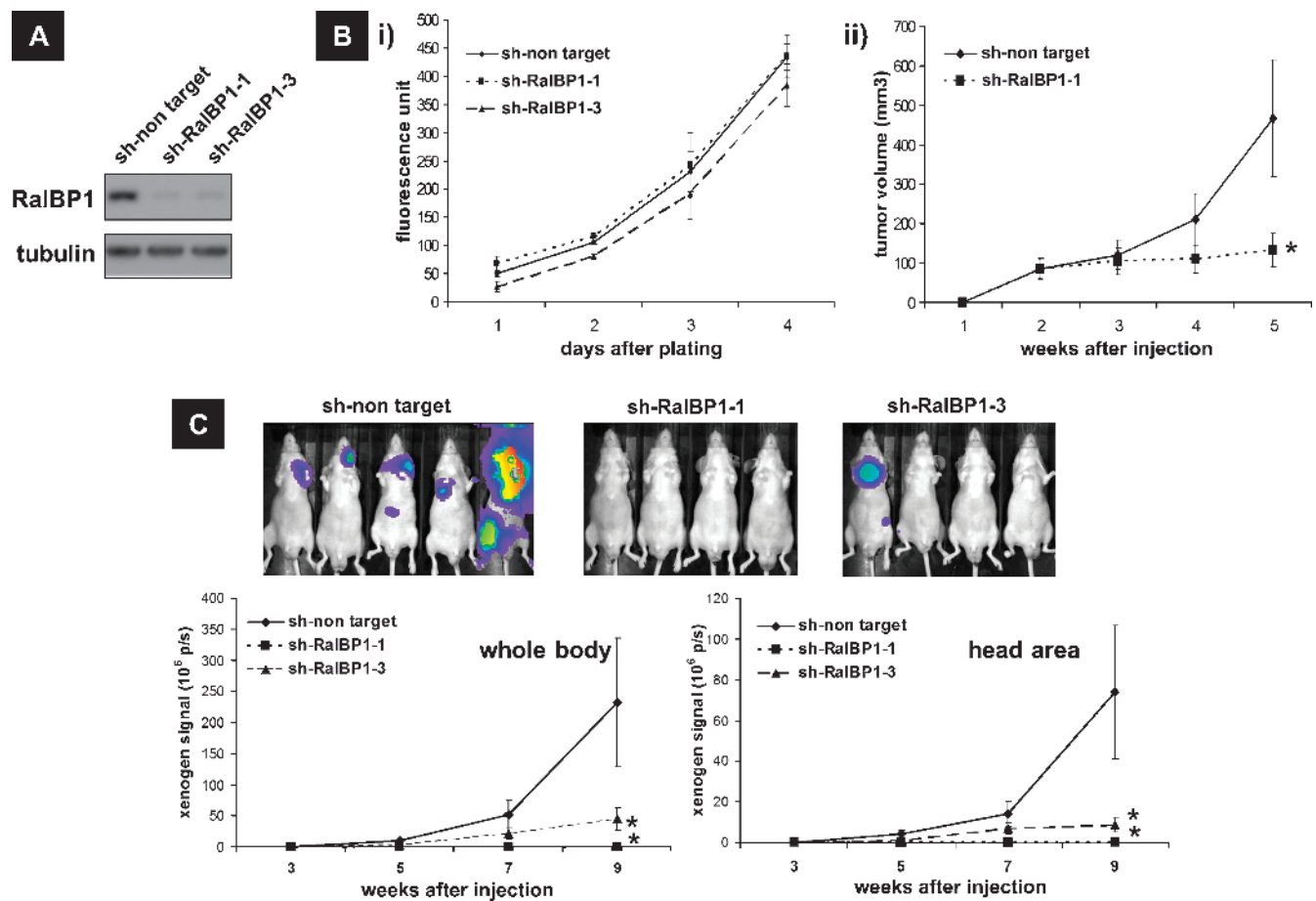


**Figure 2.** The effect of RalBP1 depletion on PC3 growth and metastasis. (A) Western blots demonstrating decreased RalBP1 protein levels in PC3 cells after infection of lentiviral-based RalBP1-targeting shRNA constructs, sh-RalBP1-1 and sh-RalBP1-3. (B) i) *In vitro* growth assessment of cells in panel A. Cell numbers were quantitated with Alamar blue at each time point. ii) *In vivo* subcutaneous tumor growth of cells in panel A. Cells in serum-free RPMI medium were mixed with Matrigel and were subcutaneously injected into the mouse flank region in five mice per group with two sites per mouse. Tumor volume was measured every week with a caliper. Error bars represent SD. \* $P < .05$  compared with sh-nontarget control at 5 weeks. (C) Xenogen evaluation of metastatic tumor growth of five mice injected with either nontarget shRNA or two different RalBP1-targeting shRNA PC3 cells. Xenogen images shown were taken at 9 weeks after injection. Graphs show quantitation of Xenogen signal at 3, 5, 7, and 9 weeks after injection. \* $P < .05$  compared with sh-nontarget control at 9 weeks. (D) Images of representative mouse mandibles dissected from mouse on necropsy. Arrows indicate where tumors are located. (E) High-resolution CT images of mouse mandibles. Dissected mouse mandibles were imaged under a high-resolution CT scanner to demonstrate bone destruction by PC3 tumors. Arrows indicate where tumors are located. (F) Xenogen evaluation of orthotopic tumor growth of six mice injected with either nontarget shRNA or RalBP1-targeting shRNA PC3 cells in mouse prostate. \*\* $P < .01$  compared with sh-nontarget control at 6 weeks. Xenogen images shown were taken at 6 weeks after injection. (G) Mouse prostate tumor size measured by a caliper at the time of necropsy at 6 weeks. \*\* $P < .01$  compared with sh-nontarget control at 6 weeks from mice described in panel F.

dilution. The Rac1 and Cdc42 activation assays were carried out according to the manufacturer's protocol (Upstate, Charlottesville, VA).

### In Vivo Xenograft Experiments

Five- to six-week-old male (for PC3 cell) or female (for UMUC3 cell) athymic nude mice (Ncr *nu/nu*) were obtained from the National Cancer Institute (Frederick, MD). Animals were maintained according to the University of Virginia ICUC guidelines. For subcutaneous or orthotopic tumorigenesis assays,  $10^6$  PC3 cells in 50  $\mu$ l of serum-free medium was mixed 1:1 with Matrigel (Becton Dickinson) immediately before injection. UMUC3 cells were suspended in serum-free medium and injected at a concentration of  $10^6$  in 0.1 ml. PC3 and UMUC3 cells were injected bilaterally into the subcutaneous flanks, and tumors were evaluated as described [14]. To evaluate the ability of

UMUC3 for lung colonization, 4-week-old female mice were injected through the tail vein with  $5 \times 10^6$  cells suspended in 0.1 ml of serum-free medium and evaluated by Xenogen bioluminescent imaging (Caliper Life Sciences, Hopkinton, MA) as described [15], and a modification of a quantitative and sensitive DNA PCR metastasis assay was described previously by our laboratory [16]. We modified the assay by use of human chromosome 12p primers and TaqMan probes. The forward primer used for human 12p was 5'-TTCACCTTTGGCA-AATGTTTATCC-3' and the reverse primer was 5'-GTGTG-GGAAGGGATTAAACC-3'. The TaqMan probe was 5'-(Hex)CCACGCAACCAGGCAA (BHQ1)-3'. To evaluate the ability of PC3 cells for metastasis,  $2 \times 10^5$  cells in serum-free medium were inoculated in the left ventricle, and bioluminescent *in vivo* imaging was used to monitor metastasis weekly. At necropsy, gross tumor areas were

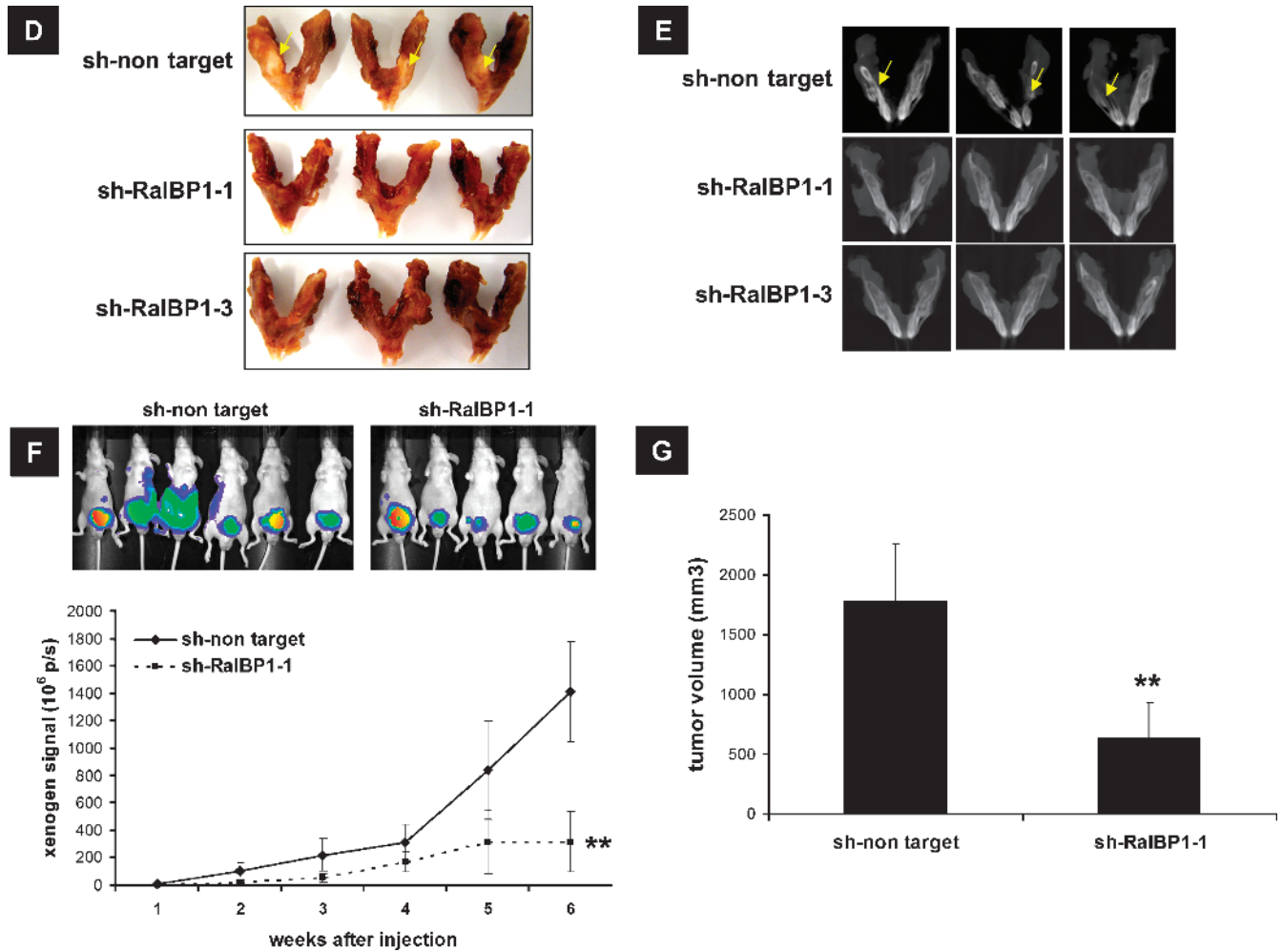


Figure 2. (continued).

dissected *en bloc* and imaged with high-resolution computed tomography (CT) to examine the bone structure.

### CT Imaging of Mice Mandibles

CT imaging of dissected tissues was performed on an open-barrel type gantry consisting of two 38-in steel wheels connected by aluminum profile pieces. The CT subsystem built for small animal imaging consists of a SourceBlock SB-80-1k x-ray source (Source Ray, Bohemia, NY) and a Hamamatsu C7940DP-03 CMOS flat panel image sensor. It was operated in  $2 \times 2$  binning mode, resulting in a  $1120 \times 1172$  detector element matrix with a  $100\text{-}\mu\text{m}$  pitch. Image acquisition and gantry rotation are controlled by a custom-written LabView program. A CT scan consisted of 400 projections, evenly spaced at  $0.5\text{-degree}$  increments over 200 degrees. This arrangement results in a total acquisition time of approximately 5 minutes. These images were preprocessed using a custom-written IDL program and reconstructed with a Feldkamp back-projection algorithm (COBRA; Exxim, Inc, Pleasanton, CA).

### Statistical Analysis

Data shown are representative of two or more experiments carried out independently. Treatment group comparisons were evaluated using Student's *t* test. Error bars are SD of the means. Values of  $P < .05$  were taken as a significant difference between means.

## Results

### Depletion of RalA Affects Prostate Cancer Cell Migration and In Vivo Growth and Metastasis

Previous studies indicated RalA but not RalB was essential for prostate cancer migration and metastasis to bone [5]. To begin determining which RalA effector was likely involved in this process, we examined the role of RalA as well as their known effectors RalBP1, Sec5, and PLD1 in cell migration. Because Sec5 and Exo84 were both components within exocyst complex, here we only evaluated Sec5. Transient transfection of siRNA duplex specifically targeting RalA, RalBP1, Sec5, and PLD1 decreased their mRNA expression level approximately 60% to 80% (Figure 1A) as evaluated by real-time RT-PCR, which was chosen in lieu of Western analysis in view of its superior quantitative reporting ability and ability to carry out comparison across several targets obviating confounders such as antibody affinity. All knockdowns were associated with a decrease in migration (Figure 1B), whereas no effect on cell number was observed for any siRNAs during the time course of the migration assay. Interestingly, depletion of RalA or RalBP1 inhibited cell migration ~60%, whereas only ~20% inhibition of cell migration was observed with Sec5 and PLD1 reduction despite similar decreased RNA levels. Because RalBP1 knockdown inhibited cell migration to a similar extent as RalA

**Table 1.** Metastasis Observed in Mice Orthotopically Injected with RalBP1 shRNA- and Control shRNA-Engineered PC3 Cells.

Cell Line (No. Mice)	No. Mice with Tumors at Site, <i>n</i> (%)		
	Kidney	Liver	Adrenal
sh-no target (6)	4 (67)	2 (33)	3 (50)
sh-RalBP1-1 (5)	0 (0)	0 (0)	0 (0)

depletion, we concluded that this effector may be an important contributor to RalA-mediated *in vivo* metastasis.

The similar effect of RalA and RalBP1 knockdown on cell migration prompted us to examine the consequences of such changes on PC3 tumor growth and metastasis. To do this, we created PC3 cells with stable knockdown of RalA and RalB (Figure 1C). Whereas depletion of either Ral protein alone had no effect on *in vitro* cell growth consistent with previous data [7], depletion of both RalA and RalB knockdown showed inhibition on subcutaneous tumor growth (Figure 1D). In contrast, RalA but not RalB significantly decreased PC3 cell bone metastasis consistent with previous reports [5] (Figure 1E).

### Reduction of RalBP1 Phenocopies the Effects of RalA Depletion on Prostate Tumor Growth and Metastasis

We also evaluated the effect of RalBP1 depletion on *in vivo* tumor growth and metastasis. The protein level of RalBP1 was decreased by ~90% after the infection of two lentiviral-based shRNA constructs targeting RalBP1, sh-RalBP1-1, and sh-RalBP1-3 in PC3 cells (Figure 2A). Decreased expression of RalBP1 had no effect on *in vitro* cell growth (Figure 2Bi). In contrast to *in vitro* growth in monolayer cultures, de-

pletion of RalBP1 significantly inhibited *in vitro* tumor growth after subcutaneous inoculation (Figure 2Bii). To assess the requirement for RalBP1 expression for PC3 metastasis, we inoculated cells infected with control and targeting shRNA constructs into the left ventricle of mice. All mice injected with nontarget shRNA cells developed metastasis 9 weeks after injection with most Xenogen signal concentrated in limbs, axial skeleton, and mandibles (Figure 2C). On necropsy, visible tumors were seen on mouse mandibles (Figure 2D), and high-resolution CT on dissected mandibles further confirmed the osteolytic destruction typically produced by PC3 metastases (Figure 2E). In contrast, none of the mice injected with RalBP1-1 shRNA-infected cells developed metastatic tumor in the 9-week period, and only one mouse showed metastasis after injection with sh-RalBP1-3 infected cells (Figure 2C).

To determine the requirement for RalBP1 expression for orthotopic prostate cancer cell tumor growth and spontaneous metastasis, we inoculated PC3 cells into mouse prostate. Depletion of RalBP1 by lentiviral-based shRNA construct, sh-RalBP1-1, reduced orthotopic tumor growth as measured by Xenogen bioluminescent signal (Figure 2F). This imaging monitored the inhibition of orthotopic tumor growth as confirmed by actual measurement of the tumor at necropsy (Figure 2G). Mice injected with nontarget shRNA cells developed liver (33%), kidney (67%), and adrenal gland (50%) metastasis at the time of necropsy (Table 1). In contrast, none of the mice inoculated with RalBP1-1-targeting shRNA cells developed metastasis in these organs, indicating that RalBP1 was necessary for PC3 cell spontaneous metastasis from orthotopic tumors.

The necessary role of RalBP1 in local tumor growth and metastasis led us to determine whether RalBP1 overexpression was sufficient to further drive tumor growth and metastasis of PC3 cells. Stable RalBP1

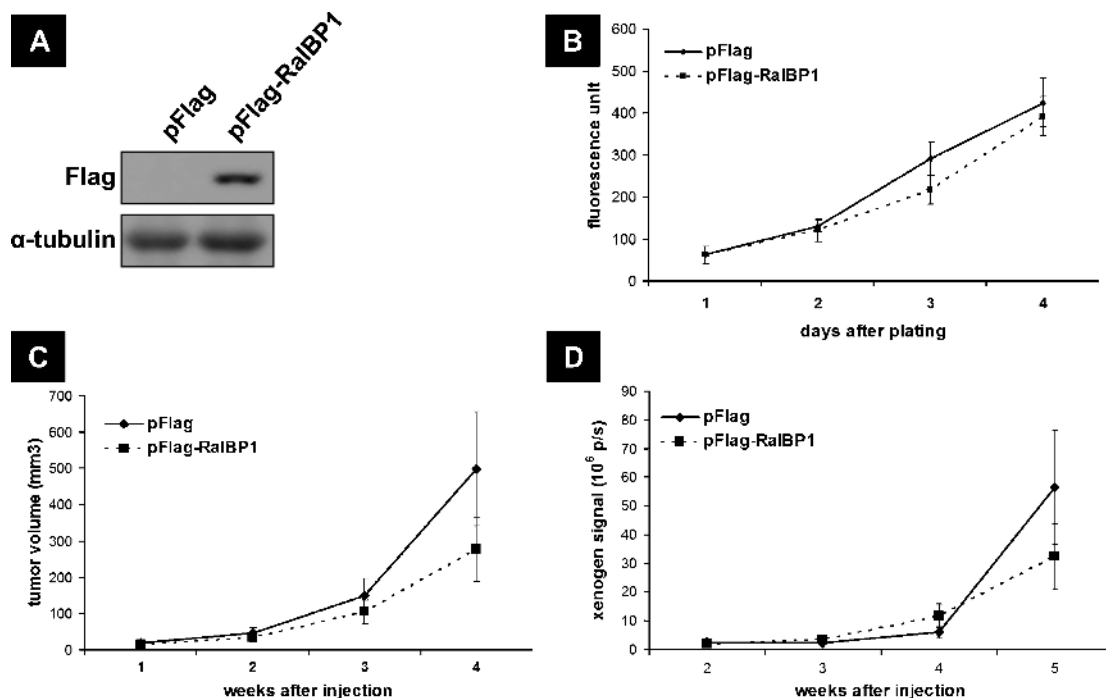


**Figure 3.** Effect of RalBP1 overexpression on PC3 growth *in vitro* and metastasis *in vivo*. (A) Western blots showing Flag-tagged RalBP1 protein level in PC3 cells after stable transfection of RalBP1 transgene used in panels B to D. (B) *In vitro* cell number as a function of time quantitated with Alamar blue. (C) *In vivo* subcutaneous tumor growth assessed by weekly tumor volume measurement in five mice per group with two sites per mouse. (D) *In vivo* metastatic tumor growth assessment using Xenogen after intracardiac inoculation as described in Materials and Methods in seven mice per group.

overexpression in PC3 cells (Figure 3A) had no effect on *in vitro* cell growth (Figure 3B) or *in vivo* subcutaneous tumor growth (Figure 3C) and metastasis (Figure 3D), suggesting that overexpression of RalBP1 alone was not sufficient to further promote these characteristics in prostate cancer PC3 cells.

#### RalBP1 Is Not the Major Mediator of RalA in Prostate Cancer Cell In Vivo Metastasis

Because depletion of RalBP1 had a similar effect on *in vivo* tumor growth and metastasis of PC3 as RalA knockdown and the former is an effector of the latter, we sought to determine the importance of RalA to RalBP1 binding in regulating PC3 metastasis. To do this, we took advantage of the D49N mutant of RalA that lost most of its binding to RalBP1 (Figure 4A), and the wild-type counterpart both made shRNA-resistant as described in Materials and Methods. These vectors were then transfected into PC3 cells stably expressing either nontarget shRNA or RalA shRNA the latter with stably reduced RalA

(Figure 4B). Western blot for total cellular RalA showed similar expression levels between shRNA-resistant wild-type and D49N mutant RalA in both nontarget and RalA shRNA-transfected cells (Figure 4B). Overexpression of wild-type or D49N mutant RalA itself had no effect on PC3 *in vivo* metastasis after intracardiac inoculation of nontarget transfected cells (Figure 4C). Depletion of RalA significantly decreased metastasis (Figure 4C) as we saw before (Figure 1E). Both wild-type and D49N mutant RalA were able to rescue the effect of RalA depletion on PC3 metastasis to a similar degree, suggesting that RalBP1 was not the primary downstream effector of RalA in maintaining metastatic competence of PC3. Supporting the notion that RalA and RalBP1 depletion may act on a different set of regulators of metastasis, such depletions led to different effects on Rac1 and Cdc42 activity. Whereas RalBP1 knockdown had no effect on Cdc42 levels or activity but increased Rac1 activity, depletion of RalA decreased both total and active Cdc42 levels and did not have a significant effect on Rac1 activity (Figure 4D).

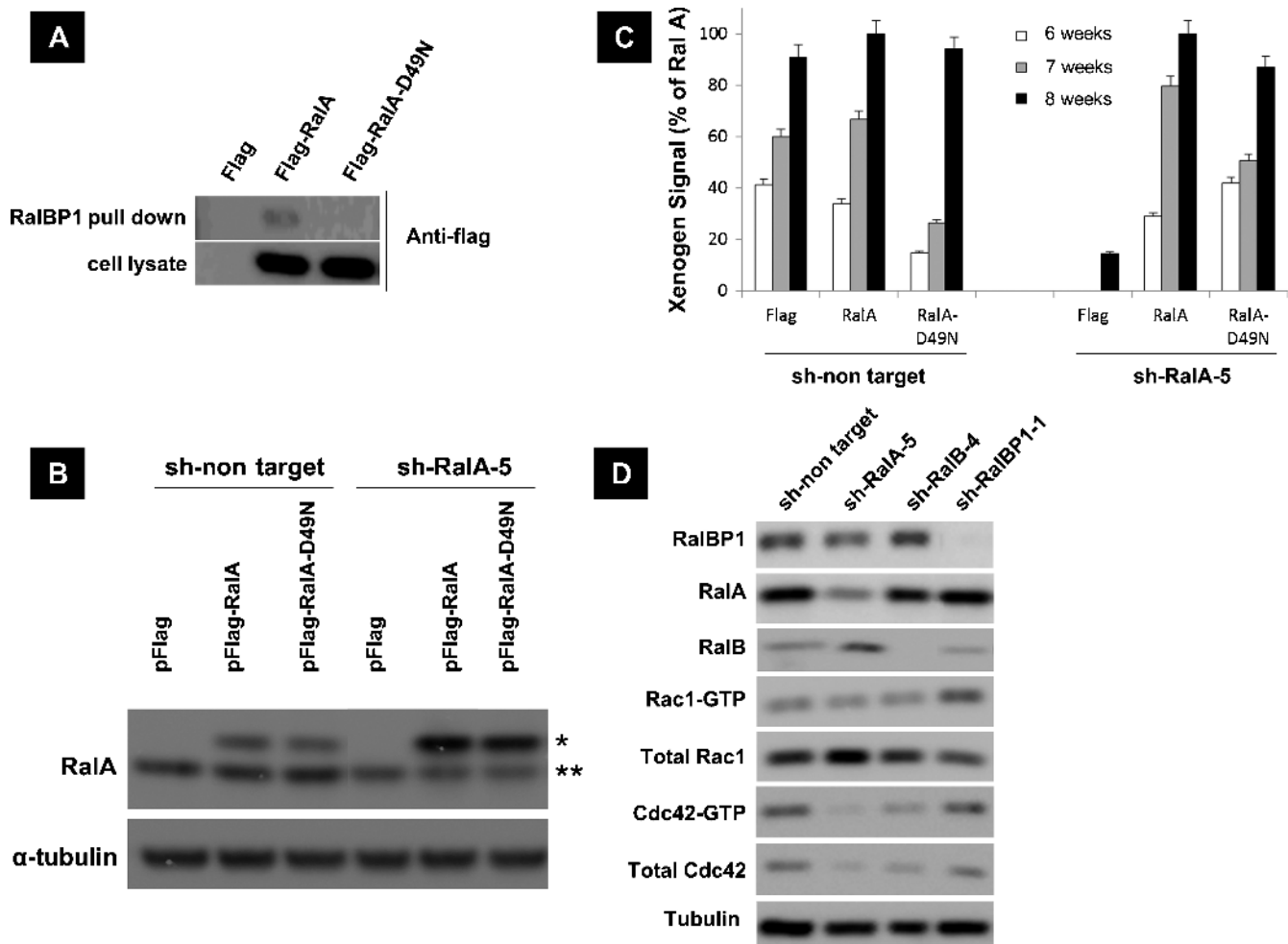


**Figure 4.** Effect of RalA to RalBP1 binding on the function of RalA in PC3 metastasis. (A) Immunoprecipitation (Flag pull-down, blot analysis with RalBP1) in transfected PC3 cells demonstrating decreased association of D49N mutant RalA to RalBP1 compared with wild-type RalA. (B) RalA protein expression levels in either control shRNA or RalA-targeting shRNA PC3 cells stably transfected with wild-type RalA and D49N mutant RalA. Wild type and D49N mutant RalA were shRNA resistant by virtue of a silent mutation as described in Materials and Methods. \*Flag tagged RalA, \*\*endogenous RalA. (C) Xenogen evaluation of metastatic tumor growth of five mice per group injected intracardiac with either nontarget shRNA or RalA-targeting shRNA PC3 cells in the context of stable expression of either wild-type RalA or D49N mutant RalA. Graphs show quantitation of Xenogen signal at 6, 7, and 8 weeks after injection. (D) Rac1 and Cdc42 activation assay in RalA, RalB, or RalBP1 depletion PC3 cells. Total lysate (10  $\mu$ g of protein) or PAK1 pull-downs (from 1 mg of protein) were Western blotted with either Rac1 or Cdc42 antibody. Results shown are typical of experiments carried out in triplicate.

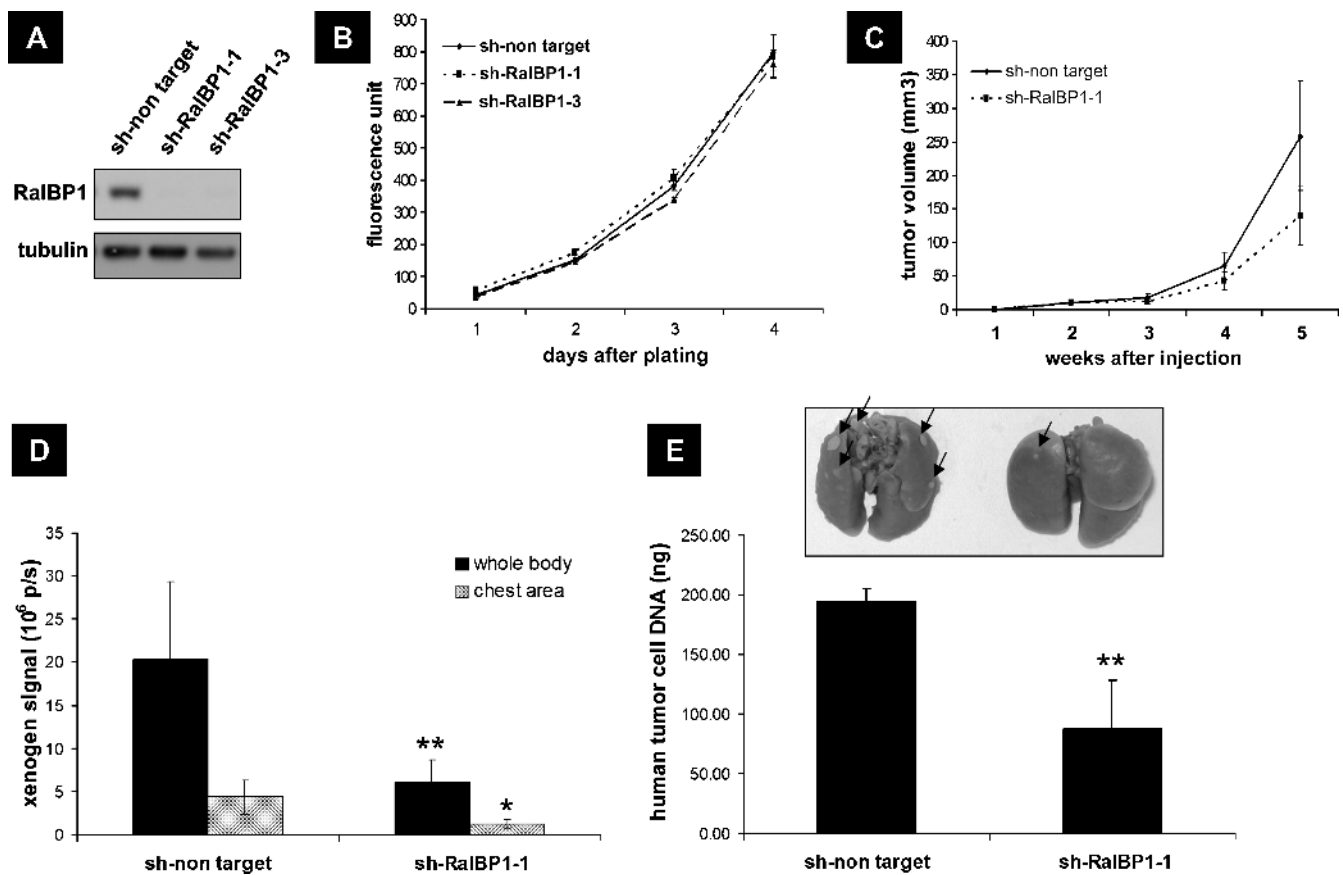


**Figure 5.** Effect of RalBP1 depletion on bladder cancer growth *in vivo* and lung colonization. (A) Western blots demonstrating diminished RalBP1 protein levels in UMUC3 cells after infection of lentiviral-based RalBP1-targeting shRNA constructs: sh-RalBP1-1 and sh-RalBP1-3. (B) *In vitro* growth assessment of cells in panel A. Cells were plated in 96-well plates with duplicate plates for each time point. Cell numbers were quantitated with Alamar blue at each time point. (C) *In vivo* subcutaneous tumor growth of cells in panel A. UMUC3 cells in serum-free RPMI medium were subcutaneously injected into the mouse flanks in five mice per group with two sites per mouse. Tumor volumes were measured weekly with calipers. (D) Xenogen evaluation of metastatic tumor growth in mice (five mice per group) tail vein injected with cells as described in panel A. Graphs show quantitation of Xenogen signal of whole body and chest area after 6 weeks of tail vein inoculation. \* $P < .05$ , \*\* $P < .01$  compared with sh-nontarget control. (E) Images of representative mouse lungs (from mice described in panel D) dissected from mouse after necropsy and fixed in Bouin solution to facilitate visualization of the tumor nodule on the surface of the lung. Mouse lungs were dissected, genomic DNA was isolated, and human-specific real-time PCR quantitation of human tumor cells in mouse lung was carried out as described in Materials and Methods. \*\* $P < .01$  compared with sh-nontarget control.

### RalBP1 Depletion Inhibits Human Bladder Cancer Lung Colonization

The observed effect of RalBP1 on prostate cancer cell tumor growth and metastasis led us to ask if the expression of this protein is also necessary for tumor growth and metastasis in other tumor types such as bladder cancer, where RalA expression is associated with higher tumor stage [7]. Bladder cancer is particularly relevant because RalBP1 is highly expressed in this tumor type at both protein [6] and RNA levels [17]. We stably depleted RalBP1 in the bladder cancer UMUC3 cell line with lentiviral-based shRNA construct targeting RalBP1 (Figure 5A). Depletion of RalBP1 in UMUC3 cells had no effect on their *in vitro* growth (Figure 5B). After subcutaneous inoculation, tumors from RalBP1 knockdown UMUC3 cells displayed slower growth rate compared with that from nontarget shRNA UMUC3 cells, but this difference did not reach statistical significance (Figure 5C). Because the major metastatic site of bladder cancer is lung, we used the lung colonization assay following the tail vein inoculation of UMUC3 cells to study the role of RalBP1 in bladder cancer metastasis. Depletion of RalBP1 in UMUC3 cells decreased metastasis as

assessed by Xenogen bioluminescent signal 6 weeks on both chest area and whole body area (Figure 5D). This finding was confirmed at necropsy using PCR for human-specific DNA in mouse lungs (Figure 5E).

### Discussion

Ral proteins were initially identified as Ras effectors of transformation. However, more recent studies have demonstrated their essential role in cancer migration and metastasis. In prostate cancer, RalA seems to be necessary for these processes [5], and the expression of this protein is associated with human tumor progression [18]. Here, we evaluated common RalA effectors for their role in human prostate cancer cell migration and identified RalBP1 as an important mediator of this process. However, whereas siRNA-mediated knockdown of Sec5 and PLD1 inhibited cell migration to a lesser extent compared with that of RalBP1 depletion, we cannot exclude them from a role in Ral-mediated cancer metastasis because cell migration is only one aspect determining the metastatic potential of cancer cells.



The similar inhibition of cell migration by RalA and RalBP1 depletion prompted us to further characterize the function of RalBP1 in RalA-dependent metastasis. Although RalBP1 depletion significantly inhibited the *in vivo* growth and metastasis of PC3 prostate cancer cells, further expression of this protein in PC3 had no effect on these phenotypes. This finding corroborated that of Awasthi et al. [19] who found that RalBP1 was essential for subcutaneous tumor growth of B16 melanomas, H358 and H520 non-small cell lung cancer, and SW480 colon carcinomas. Such findings were analogous to those with RalA that was found to be necessary for PC3 metastasis but was not sufficient to make them more aggressive [5]. This could occur if both RalA and RalBP1 are in excess compared with a limiting effector. RalBP1 depletion inhibited subcutaneous tumor growth of PC3 but not UMUC3 cells. This may be due to the different effects of this GTPase in different tumor types or may be a cell-specific effect. Similarly, RalA knockdown inhibited subcutaneous growth and metastasis of PC3, although a previous study showed that RalA depletion only had an effect on metastasis [5]. This discrepancy could be due to the different cell numbers injected. The possibility that the decrease in metastasis could result from decreased tumor growth at the primary (orthotopic) site also exists, and to determine this, one would need to compare tumors of the same size in the orthotopic location and use this to interpret the metastatic load. Our tail vein injection does not address this issue because this is a measure of metastatic colonization.

Perhaps most provocatively, although RalBP1 and RalA depletion had a similar effect on tumor growth and metastasis in PC3, the result with the D49N mutant RalA experiment pointed out that binding of RalA to RalBP1 is not required for the RalA's effect in PC3 cell metastasis. We also noted that PC3 cells with chronically depleted RalA that were transfected with wild-type RalA did not recover their full metastatic potential, although the total RalA levels were similar to cells before depletion. This finding may have several explanations. The first is that the RalA shRNA is still exerting an off-target effect on the PC3 cells that is affecting their metastatic competence without affecting other RalA-mediated *in vitro* phenotypes such as migration. Another possibility is that chronic depletion of RalA has selected cells that are not as susceptible to promotion of the metastatic phenotype by RalA overexpression. Finally, the FLAG tag may not produce a functionally equivalent RalA protein at least for the metastatic phenotype we are evaluating here.

Nevertheless, the conclusion that RalBP1 is not required for the RalA's effect on PC3 cell metastasis is further supported by the different effects of RalA and RalBP1 depletion on Rac1 and Cdc42 activity. Depletion of RalBP1 increased activity of Rac1 consistent with a previous study showing that RalBP1 has a GTPase-activating (GAP) activity toward Rac1 [20]. In contrast, RalA depletion had no effect on Rac1 activity while significantly decreasing both total and active Cdc42 levels, indicating that the effect of RalA knockdown on these proteins may not be completely mediated through RalBP1. Suppression of TBK1 or RalB has recently been shown to lead to selective lethality in KRAS-dependent cell lines [21], consistent with a previous work linking RalB through Sec5 to TBK1 activation in the setting of tumor cell survival [22]. Hence, paralog-specific effector use may be a possibility that can also explain our findings.

In contrast to these findings, there is evidence that RalBP1 is involved in transformation and tumorigenesis mediated by Aurora-A phosphorylation of RalA at S194 [23]. In addition, both Ral and RalBP1 play important roles in ligand-mediated receptor endocytosis, and the interaction between RalA and RalBP1 and their subsequent translocation to membrane was essential for this process [24]. Whereas

the dependence of these processes on the Ral-RalBP1 interaction could potentially affect *in vivo* cancer cell growth and metastasis, it may not be operative in all cases or systems (PC3) or tumor histologies (prostate).

In summary, our studies are the first to demonstrate an essential role of RalBP1 in spontaneous and experimental metastasis. This lays the foundation of RalBP1 as a promising target for therapy for this deadly form of cancer.

## Acknowledgments

The authors thank Kathleen Kelly and Gelovani Tjuvajev for the SFGnesTGL vector and Mark B. Williams for suggestions with animal imaging.

## References

- [1] Bodemann BO and White MA (2008). Ral GTPases and cancer: linchpin support of the tumorigenic platform. *Nat Rev Cancer* **8**, 133–140.
- [2] White MA, Vale T, Camonis JH, Schaefer E, and Wigler MH (1996). A role for the Ral guanine nucleotide dissociation stimulator in mediating Ras-induced transformation. *J Biol Chem* **271**, 16439–16442.
- [3] Lim KH, Baines AT, Fiordalisi JJ, Shiptitsin M, Feig LA, Cox AD, Der CJ, and Counter CM (2005). Activation of RalA is critical for Ras-induced tumorigenesis of human cells. *Cancer Cell* **7**, 533–545.
- [4] Lim KH, O'Hayer K, Adam SJ, Kendall SD, Campbell PM, Der CJ, and Counter CM (2006). Divergent roles for RalA and RalB in malignant growth of human pancreatic carcinoma cells. *Curr Biol* **16**, 2385–2394.
- [5] Yin J, Pollock C, Tracy K, Chock M, Martin P, Oberst M, and Kelly K (2007). Activation of the RalGEF/Ral pathway promotes prostate cancer metastasis to bone. *Mol Cell Biol* **27**, 7538–7550.
- [6] Smith SC, Oxford G, Baras AS, Owens C, Havaleshko D, Brautigan DL, Safa MK, and Theodorescu D (2007). Expression of ral GTPases, their effectors, and activators in human bladder cancer. *Clin Cancer Res* **13**, 3803–3813.
- [7] Oxford G, Owens CR, Titus BJ, Foreman TL, Herlevsen MC, Smith SC, and Theodorescu D (2005). RalA and RalB: antagonistic relatives in cancer cell migration. *Cancer Res* **65**, 7111–7120.
- [8] Singhal SS, Awasthi YC, and Awasthi S (2006). Regression of melanoma in a murine model by RLIP76 depletion. *Cancer Res* **66**, 2354–2360.
- [9] Singhal SS, Singhal J, Yadav S, Dwivedi S, Boor PJ, Awasthi YC, and Awasthi S (2007). Regression of lung and colon cancer xenografts by depleting or inhibiting RLIP76 (Ral-binding protein 1). *Cancer Res* **67**, 4382–4389.
- [10] Jiang H, Lu Z, Luo JQ, Wolfman A, and Foster DA (1995). Ras mediates the activation of phospholipase D by v-Src. *J Biol Chem* **270**, 6006–6009.
- [11] Min DS, Kwon TK, Park WS, Chang JS, Park SK, Ahn BH, Ryou ZY, Lee YH, Lee YS, Rhie DJ, et al. (2001). Neoplastic transformation and tumorigenesis associated with overexpression of phospholipase D isozymes in cultured murine fibroblasts. *Carcinogenesis* **22**, 1641–1647.
- [12] Ponomarev V, Doubrovina M, Serganova I, Vider J, Shavrin A, Beresten T, Ivanova A, Ageyeva L, Tourkova V, Balatoni J, et al. (2004). A novel triple-modality reporter gene for whole-body fluorescent, bioluminescent, and nuclear noninvasive imaging. *Eur J Nucl Med Mol Imaging* **31**, 740–751.
- [13] Gildea JJ, Seraj MJ, Oxford G, Harding MA, Hampton GM, Moskaluk CA, Frierson HF, Conaway MR, and Theodorescu D (2002). *RhoGDI2* is an invasion and metastasis suppressor gene in human cancer. *Cancer Res* **62**, 6418–6423.
- [14] Nicholson B, Gulding K, Conaway M, Wedge SR, and Theodorescu D (2004). Combination antiangiogenic and androgen deprivation therapy for prostate cancer: a promising therapeutic approach. *Clin Cancer Res* **10**, 8728–8734.
- [15] Wu Y, McRoberts K, Berr SS, Frierson HF Jr, Conaway M, and Theodorescu D (2007). Neuromedin U is regulated by the metastasis suppressor RhoGDI2 and is a novel promoter of tumor formation, lung metastasis and cancer cachexia. *Oncogene* **26**, 765–773.
- [16] Nicholson BE, Frierson HF, Conaway MR, Seraj JM, Harding MA, Hampton GM, and Theodorescu D (2004). Profiling the evolution of human metastatic bladder cancer. *Cancer Res* **64**, 7813–7821.
- [17] Su AI, Welsh JB, Sapinoso LM, Kern SG, Dimitrov P, Lapp H, Schultz PG, Powell SM, Moskaluk CA, Frierson HF Jr, et al. (2001). Molecular classification of human carcinomas by use of gene expression signatures. *Cancer Res* **61**, 7388–7393.

- [18] Varambally S, Yu J, Laxman B, Rhodes DR, Mehra R, Tomlins SA, Shah RB, Chandran U, Monzon FA, Becich MJ, et al. (2005). Integrative genomic and proteomic analysis of prostate cancer reveals signatures of metastatic progression. *Cancer Cell* **8**, 393–406.
- [19] Awasthi S, Singhal SS, Awasthi YC, Martin B, Woo JH, Cunningham CC, and Frankel AE (2008). RLIP76 and cancer. *Clin Cancer Res* **14**, 4372–4377.
- [20] Jullien-Flores V, Dorseuil O, Romero F, Letourneur F, Saragosti S, Berger R, Tavittian A, Gacon G, and Camonis JH (1995). Bridging Ral GTPase to Rho pathways. RLIP76, a Ral effector with CDC42/Rac GTPase-activating protein activity. *J Biol Chem* **270**, 22473–22477.
- [21] Barbie DA, Tamayo P, Boehm JS, Kim SY, Moody SE, Dunn IF, Schinzel AC, Sandy P, Meylan E, Scholl C, et al. (2009). Systematic RNA interference reveals that oncogenic KRAS-driven cancers require TBK1. *Nature* **462**, 108–112.
- [22] Chien Y, Kim S, Bumeister R, Loo YM, Kwon SW, Johnson CL, Balakireva MG, Romeo Y, Kopelovich L, Gale M Jr, et al. (2006). RalB GTPase-mediated activation of the I $\kappa$ B family kinase TBK1 couples innate immune signaling to tumor cell survival. *Cell* **127**, 157–170.
- [23] Lim KH, Brady DC, Kashatus DF, Ancrile BB, Der CJ, Cox AD, and Counter CM (2010). Aurora-A phosphorylates, activates and relocalizes RalA. *Mol Cell Biol* **30**, 508–523.
- [24] Han K, Kim MH, Seeburg D, Seo J, Verpelli C, Han S, Chung HS, Ko J, Lee HW, Kim K, et al. (2009). Regulated RalBP1 binding to RalA and PSD-95 controls AMPA receptor endocytosis and LTD. *PLoS Biol* **7**, e1000187.